RSC Advances

ROYAL SOCIETY OF CHEMISTRY

www.rsc.org/advances

For Table of Contents Only

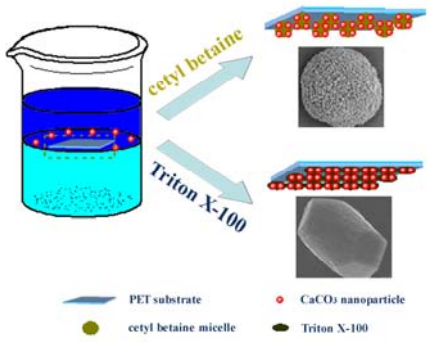

In the present work, spherical and hexagonal CaCO3 were fabricated on different surfactants micelles modified PET substrates at liquid-liquid interfaces. The results revealed a same nanoparticle-mediate self-organization process in which the surfactants act not only as the regulators but also as templates.

Cite this: DOI: 10.1039/c0xx00000x

www.rsc.org/xxxxxx

ARTICLE TYPE

Morphology Controlling of Calcium Carbonate by Self-Assembled Surfactant Micelles on PET Substrate

Zhenyou Li[a], Li Xing[a], Junhui Xiang*[a], Xiaohong Liang*[b], Chunlin Zhao[a], Huazheng Sai[a] and Fei Li[a]

Received (in XXX, XXX) Xth XXXXXXXXX 20XX, Accepted Xth XXXXXXXXX 20XX

DOI: 10.1039/b000000x

Spherical and hexagonal $CaCO_3$ with hierarchical structures were prepared on surfactant-modified PET substrate between the interfaces of saturated $Ca(OH)_2$ solution and *n*-hexane. The results show that $CaCO_3$ synthesis follows the same nanoparticle-mediated self-organization processes, but the morphology of products strongly depends on the properties of surfactant modification. The synthetic procedure offers several important characteristics for $CaCO_3$ superstructures fabrication. The surfactants in this experimental system acts not only as templates, but also as regulators for the fabrication of superstructures. This biomimetic system will be promising in synthesizing other functional nanoparticles or nanodevices.

Introduction

Hierarchical structure of biomaterials that exhibit uniform morphology and outstanding mechanical properties are universal in living organisms.[1] One secret of biomaterials' superior properties is their organic-inorganic hybrid structure whereby precise arrangement of building blocks is achieved over several length scales.[2] The organic components, biomacromolecules and organic matrices, can regulate crystal nucleation and growth, modulate crystal shape and size, and control the organization of building blocks into complex structures, having been an active area of research during the past few years.[3-5]

Calcium carbonate is one of the most abundant biomaterials in nature, mainly as exoskeleton in shells and cell walls or as mechanical support in spicules and spines,[1] exhibiting different structures and properties to carry out specific functions respectively. Its crystal structure, size, and shape are the major concerns in crystallization, and have recently received a great deal of attention. Many efforts have been made to mimic the biomineralization process in order to prepare $CaCO_3$ crystals with defined characteristics.[5-7] These biological strategies can be concluded into two categories: (1) mineralization in insoluble matrices such as polymeric scaffolds[8], biopolymer gels[9-11] or self-assembled monolayers (SAMs)[12-14], (2) crystal growth with the help of soluble additives such as polymers[15], copolymers[16], or surfactants[17]. And the latter soluble molecules are believed to participate in both the nucleation and growth processes by either binding selectively to certain families of crystal planes[18, 19] or interacting with the charged ions to stabilize the unstable phases[20], which are thought to be an effective and versatile method. Therefore, most researchers put emphasis on finding new molecules with regulating effect and how the regulating effect works. For instance, calcium carbonate crystal with spiky dumbbell-like superstructure was synthesized in the presence of casein, a typical phosphoprotein.[21] Wei et al. used a non-ionic peptide type block copolymer as the structure-directing agent to produce calcite with stepped (104) face at the air-solution interface.[16] In most of the works, the soluble additives are present in the form of molecules. However, these amphipathic molecules are easy to assemble to different shapes of micelles. And the micelle itself is a good template. So these micelles are better candidates to regulate the shape of $CaCO_3$ crystals. But there have been very few researches using soluble additive micelles to direct the growth of the crystals.[22, 23]

As most of the crystallizations take place in solution, the biggest problem to this issue is the dynamic nature of the micelles in solution. The shape of the micelles in solution is strongly affected by the solution environment. As the time changing, the properties of the solution where the crystallization reaction happens are also changed. Thus, the shape of the micelles is different. Even the micelles may disappear. Compared with bulk solution, solid-liquid interface provide a unique environment for additive molecules assembly. The assembled patterns are mainly determined by the substrate and additive properties (such as hydrophobic property, surface charge density), which are always different from those in free solution.[24-28] This makes it possible to control the morphology of crystals by anchoring the self-assembled micelles on solid substrate.[29-31]

In the previous study, [14] we revealed the basic rules of forming the superstructure materials via a nanoparticle-mediated self-organization process. We found that the synergetic effects between the organic-inorganic interfaces and the self-assembled monolayers (SAMs) are the essential factors for the control of the hierarchical structures. The SAMs can induce the directions and arrangement of the building blocks. Indeed, the regulation effect of the substrate will be enhanced if the surfactant micelles are further modified on the SAMs. The stronger effect of the surfactant micelles modified substrate relies not only on the

larger amount of functional groups, but also the template effect of the micelles.

Therefore, in this work, the regulation effects of the surfactant micelles modified poly (ethylene terephthalate) (PET) substrate on $CaCO_3$ morphology were studied. And spherical and hexagonal $CaCO_3$ hierarchical structures were produced respectively when cetyl betaine and Triton X-100 were induced. Herein, the organic-inorganic interface provides an independent synthetic environment from bulk solution. The surfactants act not only as structure-directing agents inducing the orientation of the particles, but also as templates guiding them to the final morphology. In both conditions, the formation of $CaCO_3$ hierarchical structures follows the same nanoparticle-mediated self-organization process, which provides us with a facile way to produce hierarchical nanomaterials with defined structures.

Experimental

Materials

Calcium hydroxide, ammonium bicarbonate, n-hexane, ethanol, acetone, toluene and p-octyl polyethylene glycol phenyl ether (Triton X-100) were purchased from Beijing Chemical Reagents Company. Aminopropyl triethoxysilane (APTES) was purchased from Alfa Aesar. Octadecyltrichlorosilane (OTS) was purchased from Acros Organics. Cetyl betaine was purchased from Chem Service Company. All chemicals were of analytical grade and used as received without further purification. All the glassware was cleaned by sonication in water for 5 min, and rinsed with distilled water, finally dried at 105 °C.

Fabrication of hydrophobic and hydrophilic surface of the polymer substrate

By assembling octadecyltrichlorosilane (OTS) on PET substrate, the hydrophobic surface of PET substrate was fabricated according to references[32-34]. In a typical experiment, APTES was dissolved in acetone (1 vol%) and aged for 240 h. PET substrate was ultrasonically cleaned for 5 min successively in distilled water, ethanol, and acetone and then dried at 105 °C for 5 min. The dried substrate was immersed in the acetone solution of APTES for 5 min and baked at 105 °C for 5 min to form a buffer layer. After that, the substrate grafted by buffer layers was immersed in the OTS solutions (1 vol % in toluene) under a nitrogen atmosphere for 2 min and then rinsed with anhydrous toluene and baked at 105 °C for 5 min to form the hydrophobic surface of PET substrate. The hydrophilic surface of PET substrate was obtained by irradiating the hydrophobic PET substrate with ultraviolet (UV) light. The UV-irradiated surface became hydrophilic because of the formation of hydroxyl groups.

Self-assembly of surfactant on the modified PET substrate

The PET substrates with hydrophobic/hydrophilic surface were immerged in the saturated solution of surfactant for 30 min at 80 °C, and slightly rinsed with deionized water, then dried at 105 °C. In this way, the surfactant molecules assembled at the solid-liquid interface. Here, the cetyl betaine and Triton X-100 were chosen for the study.

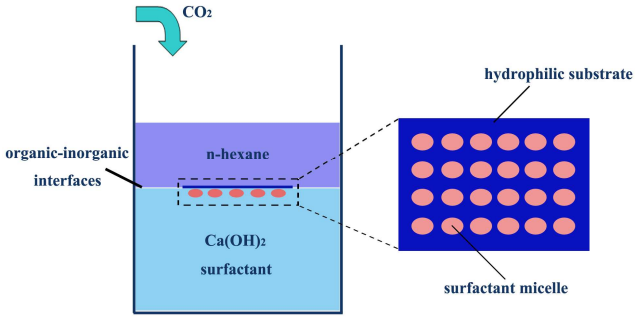

Scheme 1. Design of the experiment. Surfactant micelles modified substrate was put at the organic-inorganic interface with the modified side towards the inorganic phase. CO_2 came from the decomposition of NH_4HCO_3.

$CaCO_3$ growth on the surfactant-assembled substrate

Room-temperature mineralization of $CaCO_3$ on the PET substrate was performed at the organic-inorganic liquid interface by a slow gas-diffusion procedure. The organic phase was n-hexane while the inorganic phase was $Ca(OH)_2$ saturated solution with 500 μL saturated surfactant solution. The nucleation and growth of $CaCO_3$ were induced by carbon dioxide from the decomposition of NH_4HCO_3 diffusing into the system. (Scheme 1) After a period of time, the substrates covered with $CaCO_3$ were taken out, and the overgrown specimens were slightly rinsed with deionized water. Then the as-grown $CaCO_3$ on the substrate was dried in air for further characterization.

Characterization of $CaCO_3$ Deposited on the substrate

The processes of silane and surfactants self-assembly were characterized by water contact angle through JC2000C1 (POWEREACH). The small pieces of as-prepared $CaCO_3$ on the modified PET substrates were coated with gold for scanning electron microscopy (SEM) measurements on a JMS-6301F microscope. An X-ray diffractometer (XRD, MSAL XD-2 powder X-ray diffractometer), operating at 30 kV, and a current of 30 mA with Cu Kα radiation, λ=1.54056 Å, also was used for characterizing the samples. Infrared spectroscopic analysis was performed in transmission mode (FT-IR) using a VERTEX 70, with scanning from 4000 to 500 cm^{-1}.

Results and Discussion

Surfactant assembly on the PET substrate

In this research, zwitterionic surfactant cetyl betaine and nonionic surfactant Triton X-100 were chosen to modify both the hydrophilic and the hydrophobic substrates. The surface properties of substrates were characterized with the water contact angle device. And the results are shown in Figure 1. The contact angles of cetyl betaine micelles modified hydrophilic substrate and Triton X-100 one are 5° and 7° respectively. Comparing with the hydrophilic surface of blank PET, the contact angle became smaller after assembling either cetyl betaine or Triton X-100. While for the hydrophobic substrates, the contact angle did not change after surfactants assembly, still remaining 105°.

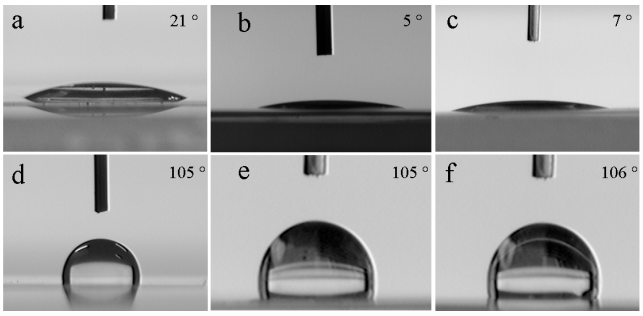

Figure 1. Water contact angles (°) of surfactant micelles assembled substrates and the blank substrates. a) the hydrophilic surface of blank PET; b) the cetyl betaine micelles were assembled on the hydrophilic surface; c) Triton X-100 micelles were assembled on the hydrophilic surface; d) the hydrophobic surface of blank PET; e) cetyl betaine was assembled on the hydrophobic surface; and f) Triton X-100 was assembled on the hydrophobic surface. The contact angle value was shown on the top right corner of each figure.

The drop of the contact angle of the modified hydrophilic substrates results from the change of the functional groups on the surface, indicating the formation of the surfactant micelles on the substrate. In the saturated aqueous solutions, whose concentrations were above the critical micelle concentration (CMC), surfactants existed almost in the form of micelles, with head groups outward to form hydrophilic membrane. Since the head groups of surfactant have a strong affinity to the hydrophilic substrate, the micelles could be assembled onto the substrate easily when the substrate terminated with hydroxyl groups is immerged into the saturated aqueous solutions of surfactants.[35-37] Figure 2 shows the SEM images of PET substrate before and after modification. Before modification, both the hydrophilic and hydrophobic substrates have a smooth surface. The bright spots on the substrates are the sputtered Au nanoparticles. After modification, cetyl betaine micelles and Triton X-100 micelles are formed only on the hydrophilic substrates. Figure 2b shows cetyl betaine micelles modified substrates are spherical while the Triton X-100 micelles have spindle morphology as shown in Figure 2c. What should point out here is that since the drying process will affect the micelle structure, the SEM images may not reflect the structures formed in situ. Although the SEM data is speculative, these surfactant aggregates on the substrates also suggested a successful modification. Given the experimental results mentioned above, we proposed a possible modification process with detailed description which was shown in Figure 3. After the assembly of cetyl betaine micelles, the terminal groups of the substrate become -COO^- while the surface groups of the blank PET are hydroxyl. The difference between the deprotonated carboxyl groups against hydroxyl groups benefits the improvement of hydrophilicity, and the water contact angle become smaller. When it comes to Triton X-100, the surface groups are still hydroxyl. But as the assemblies of the micelles, more hydroxyl groups are formed on the surface of the substrate. Thus the modified substrate has a denser hydroxyl groups than that of the blank PET, becoming a more hydrophilic substrate.

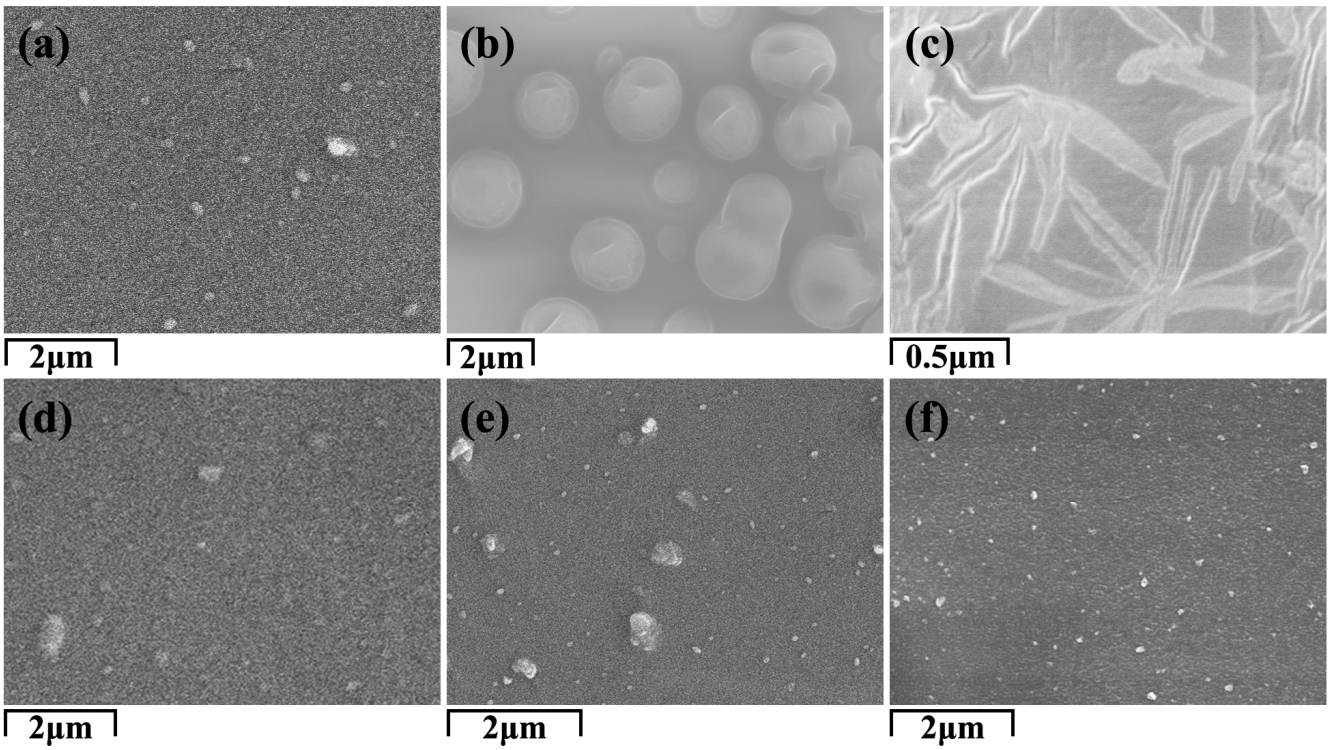

Figure 2. SEM images of hydrophilic PET (a), treated with cetyl betaine (b) and Triton X-100 (c). SEM images of hydrophobic PET (d), treated with cetyl betaine (e) and Triton X-100 (f).

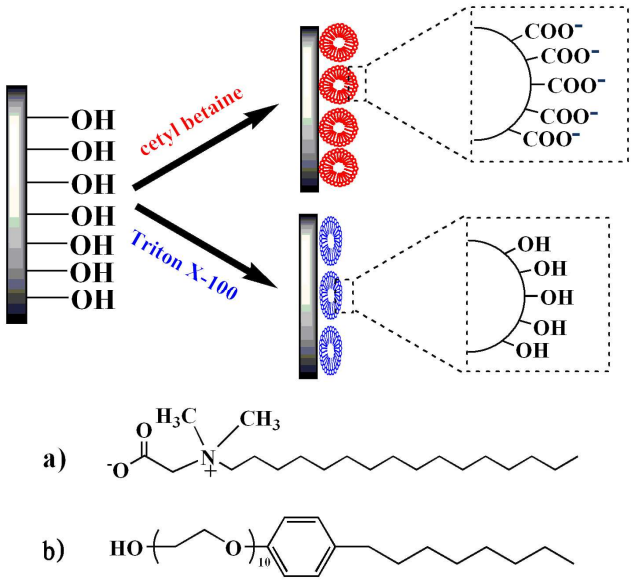

Figure 3. The formation of surfactant micelles on the hydrophilic substrates. a) The molecular formula of cetyl betaine; b) the molecular formula of Triton X-100.

And the water contact angle reduces.

The final state of surfactants aggregates was a balance of the interactions between surfactant, solvent, and a solid substrate on the aggregation. To make it simple, we have studied only net neutral surfactants. (For zwitterionic surfactant cetyl betaine, the negative charged carboxyl was neutralized by quaternary ammonium cation.) The strong monopolar charge-charge interactions that occur for anionic or cationic surfactants were minimized. Under this condition, the surfactants aggregates were more strongly affected by solution conditions, substrate property and neighboring aggregates.[30] In this research, the authors chose saturated aqueous solutions for the surfactant assembly in which the concentration was higher than that of the bulk CMC. Therefore, most of the surfactant in solution formed spherical aggregates, and the surfactant micelles' morphology was no longer a function of concentration. Herein, the difference between the assembled aggregates of cetyl betaine and Triton X-100 was contributed to their different head groups. So, it is reasonable to consider the structure change of the micelles from solution to substrate due to the replacement of water-headgroup interactions with surfactant-solid interactions. There is a correlation between the surfactant curvature and the affinity of the head group for the solid substrate. On the one hand, a high density of surface sites that can form strong bonds between the head groups and the substrate will lead to a strong perturbation of micelle structure. Thus a less curved micelle would form as the density of available strong-bonding sites increases. As for Triton X-100, its head groups are hydroxyl, which can hydrogen-bond with the hydroxyl groups on the substrate. This strong interaction may be the main contributor to the structural change after assembling. It is therefore, the curvature becomes smaller, forming the spindle-shaped surfactant micelles on the substrate. On the other hand, if the substrate forms low energy bonds with the surfactant head groups, it is reasonable to have slightly perturbed micelles attached to the solid. The head groups of cetyl betaine are carboxyl groups and quaternary ammonium cations, which can interact with the substrate also by hydrogen bonds. But the hydrogen bonds between the cetyl betaine and the substrate are weaker than that of the Triton X-100. This relatively weak interaction would not change the shape of the micelles after assembling, maintaining spherical. Furthermore, the repelling interaction between carboxyl groups causes the distances between the cetyl betaine aggregates units larger than that of Triton X-100 (Figure 2b~c).

While for the hydrophobic substrates, the contact angle had nearly no change after immerging into the surfactant saturated aqueous solutions (Figure 1d~f). There was an alkyl chain layer on the surface of the OTS-modified hydrophobic substrate, so that the solid substrate cannot form hydrogen bonds with the surfactant head group. In this situation, a large free energy reduction of the system was possible by covering up the solid substrate with surfactant hydrocarbon tails. So the free surfactant monomers or hemicylinder micelles could be assembled onto the substrates by the hydrophobic interactions.[37] However, the results showed that the water contact angle of hydrophobic substrate was not changed. The SEM images of this kind of substrate before and after treating with surfactant solutions (Figure 1d~f) had also shown that the assembly of surfactants did not take place. This indicated that there were few free surfactant monomers or hemicylinder micelles in the saturated solutions, and the reduction of free energy was not sufficient to perturb the structure of spherical micelle in the bulk solution.

It is worth noting that surfactant micelles can only self-assembled on hydrophilic substrate. Since the hydrophilic substrates were obtained by irradiating the hydrophobic PET substrates with UV light. If we expose only one side of the substrate to UV light, this side becomes hydrophilic while the other side keeps hydrophobic. When the substrate was immerged into surfactant solution, the micelles assembled only on the hydrophilic side, and the other side remained hydrophobic. The amphipathy of the substrate allows it to float between the organic-inorganic interfaces, which make the following study possible.

Morphology of $CaCO_3$ on the substrates

Cetyl betaine and Triton X-100 surfactant micelles modified substrates were put at the organic-inorganic interface separately with the hydrophilic side towards the aqueous phase. After 48 hours of reaction, different shapes of $CaCO_3$ crystals were grown on these substrates respectively. When cetyl betaine micelles modified substrates were induced in the reaction system, spherical particles with about 30μm in diameter were fabricated (Figure 4a). The inset picture of Figure 4a is the low-magnification image of $CaCO_3$ samples, which shows that the samples are composed of a large quantity of well-dispersed spherical particles with uniform diameter. The surface appearance of sphere was clearly visible in Figure 4c, showing triangular pyramidal morphology radiating from the centre of the crystals. These pyramids were 1μm height with similar shape and smooth surfaces. The typical image of the cracked sample in Figure 4d shows that the $CaCO_3$ spheres are composed of some small sticks. And we should also notice the hole (indicated by the black arrow) in the centre of the cracked sphere suggesting a core in the spherical crystal. The size of the hole is about 1-2μm which is just the same as the size of the cetyl betaine micelle. These results

reveal that the micelles have a template role in the growing process. More detailed information about the spherical structure can be further provided by XRD analyses. In Figure 4b, the XRD spectrum clearly indicates that the as-prepared products are composed of a calcite phase with the characteristic (104), (110), (113), (202) and (116) planes (JCPDS card No. 05-0586). The two broad peaks observed at 47.2 ° and 54.1 ° were consistent with the XRD pattern of blank PET shown in Figure S1. The random orientations of the crystals suggest that cetyl betaine molecules have relative weak interaction with the planes of calcite crystals. Thus, the adsorption on specific planes did not take place. Controlled experiment was taken when cetyl betaine micelles modified substrate was removed from the system. The obtained products showed a rhombohedral calcite phase with an average size over 50μm (Figure S2), revealing the surfactant has an important influence on the morphology of $CaCO_3$.

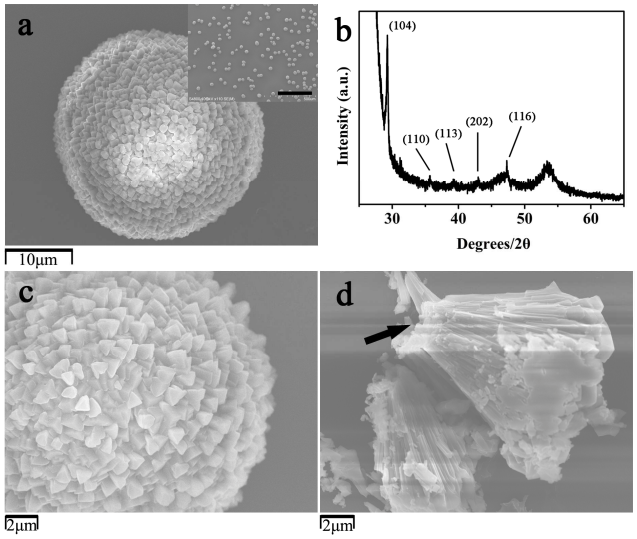

Figure 4. a, c, d) The typical SEM images and b) corresponding XRD pattern of $CaCO_3$ which were fabricated on the cetyl betaine-assembled hydrophilic substrate between the *n*-hexane-aqueous interfaces. The inset in (a) is the low-magnification image of the specimen presented in Figure 2a.

On the other hand, the introduction of Triton X-100 micelles onto the substrate resulted in the formation of hexagonal $CaCO_3$ crystals. In Figure 5a, the hexagon was 4μm in length and 3μm in width. The inset picture of Figure 5a shows a large number of hexagonal $CaCO_3$ with high nucleation densities and narrow spread particle size on the substrate. The rough surface of the hexagonal crystals can be seen at high magnification in Figure 5c~d. The corresponding XRD spectrum in Figure 5b indicated that the as-synthesized products were composed of a calcite phase with the characteristic (104) and (202) planes. Similarly, the two broad peaks at 47.2 ° and 54.1 ° belonged to blank PET (Figure S1). Without the Triton X-100 micelles, $CaCO_3$ crystals grow in random directions resulting in many other planes in the XRD curve. [14] This means Triton X-100 molecules have strong interaction with the (104) and (202) planes. When absorbing on the planes, they can inhibit the crystals from growing vertical to the directions. Thus these planes are remained while others disappeared. $CaCO_3$ that mineralized without Triton X-100 results in the formation of large rhombohedral calcite crystals with an average size over 50μm (Figure S2), revealing the surfactant has a significant influence on the crystalline $CaCO_3$.

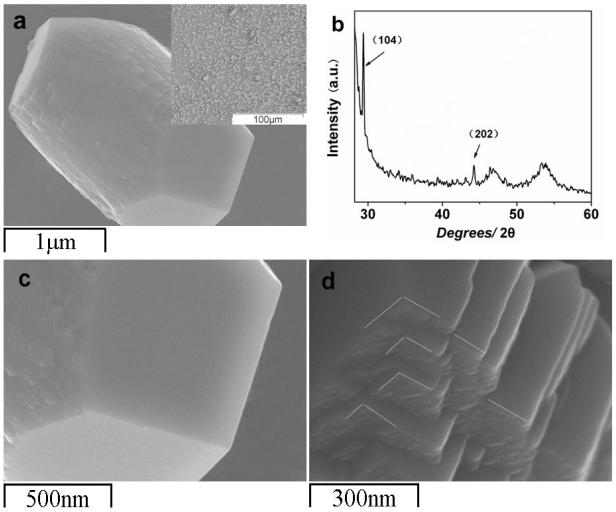

Figure 5. a, c, d) The typical SEM images and b) corresponding XRD pattern of $CaCO_3$ which were fabricated on the Triton X-100-assembled hydrophilic substrate between the *n*-hexane-aqueous interfaces. The inset in (a) is the low-magnification image of the specimen presented in Figure 3a.

Both the spherical and hexagonal products are different from those obtained from the organic-inorganic interface. In addition, $CaCO_3$ crystals grow evenly on the hydrophilic side of the substrate. While on the hydrophobic side, we can only find very few rhombohedral crystals at the edge of the substrate. All these evidence shows that the surfactant micelles modified substrates play a key role in modulating the morphology of the crystals.

The roles of surfactant on $CaCO_3$ morphology

To further demonstrate the important role of the surfactant, the morphological development of $CaCO_3$ at different crystallization times was examined. The representative SEM images of the products obtained at 2h, 12h, 24h and 48h are presented in Figure 6 and Figure 7.

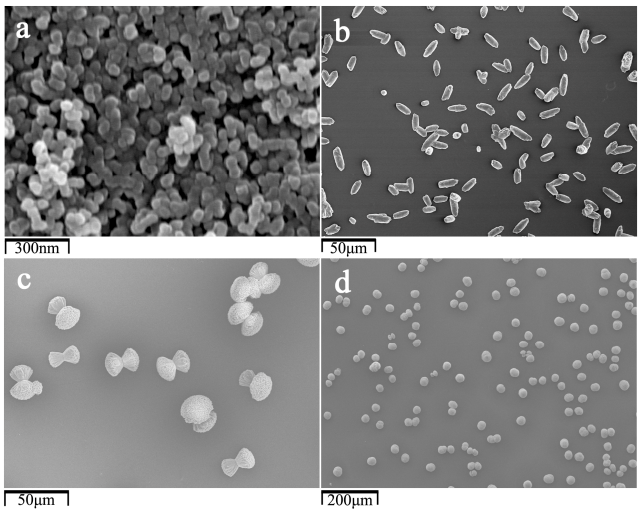

Figure 6. a) SEM image of the products obtained directly from the organic-inorganic interface (not on the substrate) after crystallization for 2

h; b, c, d) SEM images of $CaCO_3$ prepared on the cetyl betaine-assembled substrate for 12 h, 24 h and 48 h respectively.

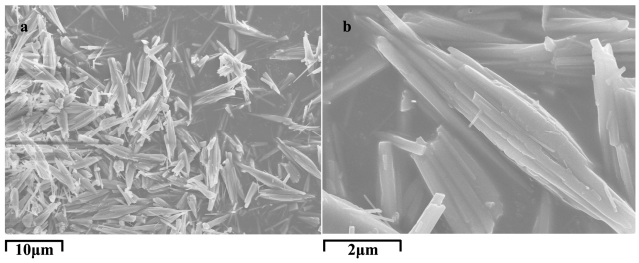

Figure 7. SEM images of rod-like $CaCO_3$ crystals obtained from the substrate free system. The surfactant in the inorganic phase is cetyl betaine.

Figure 6 shows the whole growing process when cetyl betaine was induced in the system. The products of Figure 6a were collected directly from the organic-inorganic interfaces (not on the substrate) after 2h of reaction. It is clear that the first species to form are amorphous calcium carbonate sphere particles with about 50nm in diameter. This is in good agreement with previous works. [14, 38, 39] When the reaction time is prolonged to 12h, the as-prepared products are rod-like crystals with 20μm in length and 5μm in diameter. When crystallized for 24h, sheaf-like $CaCO_3$ hierarchical structures appear. Finally, spherical $CaCO_3$ crystals are formed. The whole process of the crystals growth on the substrate is just like flowers in bloom. In addition, the size of the crystals did not change from 12h to 48h, which means the further growing process is just the continually assembly of the building blocks. This result also reminds us of the earlier findings in Figure 4d that the $CaCO_3$ spheres are composed of small sticks. To obtain more evidence for the formation of these building blocks, the morphology of $CaCO_3$ grown in the same but substrate free system was examined. In this system, the modulate effect of the functional substrates was removed, but the surfactant in the aqueous phase will still regulate the crystal growth. The corresponding images in Figure 7 show the products have the similar size and shape to that of the building blocks. This is direct evidence that the $CaCO_3$ sticks which finally assembled into spherical $CaCO_3$ hierarchical structure was formed with the help of the surfactant in the aqueous phase.

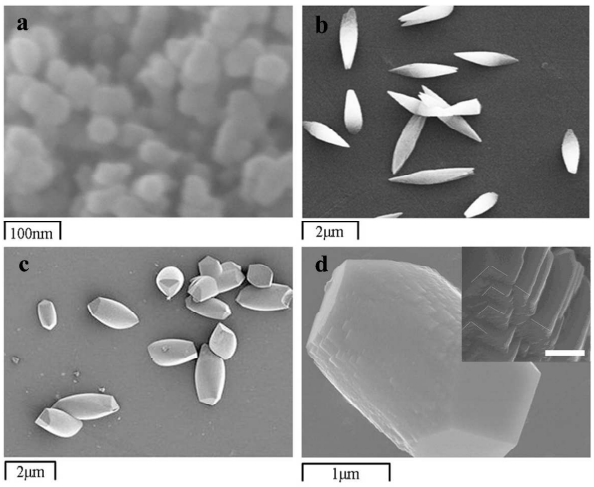

Figure 8. a) SEM image of the products at the n-hexane-aqueous interface after crystallization for 2 h; b, c, d) SEM images of $CaCO_3$ prepared on the Triton X-100-assembled substrate for 12 h, 24 h and 48 h respectively. The scale bar of the inset in (d) is 300 nm.

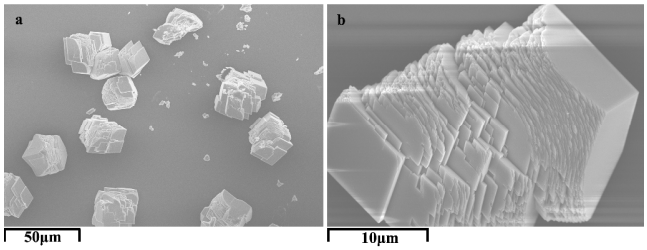

Figure 9. SEM images of rod-like $CaCO_3$ crystals obtained from the substrate free system. The surfactant in the inorganic phase is Triton X-100.

When it comes to the Triton X-100-modified substrate, the growth of the hexagonal $CaCO_3$ followed a similar process. Figure 8a shows the microstructure of $CaCO_3$ obtained from the organic-inorganic interface (not on the substrate) after 2h of crystallization. It can be seen that the products are consisted of 30nm nanoparticles, revealing that the early stage of the hexagonal products are also amorphous calcium carbonate. With the time passing, spindle-shaped and hexagonal $CaCO_3$ were fabricated on the substrate. Comparing Figure 8b-d, we can find a smooth surface is gradually forming at the end of the spindle, which reveals a ripening process in the crystal growth. In order to get more details about the formation mechanism, we construct a same but substrate free system. After 24h of reaction, calcite crystals with layered structure have been found as shown in Figure 9. It is worth noting that the products grown on the Triton X-100 micelles modified substrate (Figure 5d) have similar structures, which means the surfactant molecules in the solution play a significant role in forming the structure and morphology of the hexagonal $CaCO_3$. And this layered structure comes from the specific adsorption of Triton X-100 on (104) and (202) planes (see the XRD pattern in Figure 5b).[4, 16]

Besides, in both conditions, the density of the crystals on the substrates is high in the edges while low in the middle. This phenomenon reveals $CaCO_3$ growth begins from the edges of the substrates, also indicating a self-organization process on the substrates.

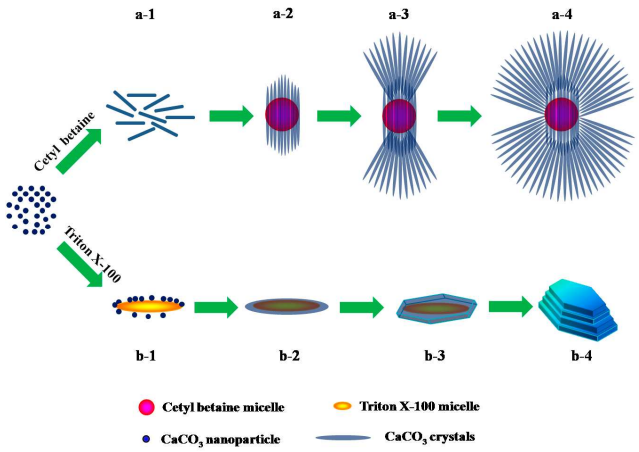

Scheme 2. The possible formation process of $CaCO_3$ crystals on cetyl betaine micelles modified substrate (a-1~a-4) and Triton X-100 micelles modified substrate (b-1~b-4).

Based on the experiment results mentioned above, it could be suggested that $CaCO_3$ synthesis follows the same nanoparticle-mediated self-organization processes. However the final morphology of products depends on the shapes of the micelles on the substrate. Scheme 2 shows the possible formation process of $CaCO_3$ crystals. At the very beginning of $CaCO_3$ growth, carbon dioxide from the decomposition of ammonium bicarbonate reacted with H_2O to enrich the carbonate ions and then induce heterogeneous precipitation to form nanoparticles between the organic-inorganic interfaces. In this process, the terminal groups of the surfactant in the aqueous solution may affect the particles formation. As for cetyl betaine, the deprotonated $–COO^-$ groups have the ability to bind calcium ions by electrostatic interaction. After that, these nanoparticles are likely to transfer to the substrate, interacting with the surface groups of the cetyl betaine micelles through electrostatic interactions, hydrogen bonds or Van der Waals forces. At the same time, these nanoparticles with random crystallographic orientations and high internal energy are growing gradually to fuse with each other and tending to lower the energy by arranging orderly and assembling into $CaCO_3$ sticks (Scheme 2 a-1). Consequently, these sticks may rotate to get the same orientation with driving force coming from specific absorption of the surfactant and the removing of surface energy which is shown in Scheme 2 a-2.[40] Meanwhile, some other $CaCO_3$ nanoparticles attach to the sticks by Brownian motion and form more sticks in the same manner. With an increasing of crystallization time, these building blocks (the sticks) begin to aggregate at both ends of the $CaCO_3$ nanorods. (Scheme 2 a-3) Finally, $CaCO_3$ hierarchical structures with unusual morphologies are formed by continually attaching sticks or nanoparticles. (Scheme 2 a-4) When cetyl betaine is replaced by a nonionic surfactant (Triton X-100), $CaCO_3$ growth suffers the same process. CaCO3 nanoparticles formed at the interfaces will transfer to the substrate and absorb on the micelles. (Scheme 2 b-1) These nanoparticles tends to fuse with each other and crystallize into hexagonal calcite crystals. (Scheme 2 b-2~b-3) At this time, surfactant molecules (Triton X-100) in the saturated $Ca(OH)_2$ solution may have strong interaction with some specific planes of $CaCO_3$ and absorbed on these planes. So the crystal growth along this direction will be constrained. When other nanoparticles absorbed on the hexagonal crystals, they can only grow vertical to this direction. Finally, hexagonal CaCO3 crystals with layered structure are formed after hours of reaction.

For most of the time, the balance between the crystal growth and mass transport is an important factor in controlling the morphology of crystals. But herein, the surfactant micelles assembled on the substrate play the leading role in influencing the final morphologies. And the size of $CaCO_3$ crystals is also affected by the micelles. The cetyl betaine micelle (Figure 1b) has a bigger size than the Triton X-100 micelle (Figure 1c). Then, after crystallization, the spherical $CaCO_3$ flowers (Figure 4a) are therefore bigger than the hexagonal crystals (Figure 5a). Moreover, the surfactant micelles in the biomimetic mineralization system are acting not only as a template, but also as an inhibitor preventing $CaCO_3$ crystallizing. In the FTIR spectra (Figure 10), the presence of the peak at 1082 cm^{-1} attributed to symmetric stretch of carbonate ion in plane (ν_1), and the split peaks at around 1387 could be seen as its asymmetric stretch in plane (ν_3) which can be indexed as the characteristic peaks for amorphous calcium carbonate (ACC). [7, 21, 41, 42] This result is consistent with our previous work [14] that nanoparticles obtained by an ACC-to-calcite transformation. It also shows that the surfactant micelles have the ability to stabilize ACC as ACC can be found even after 48h mineralization.

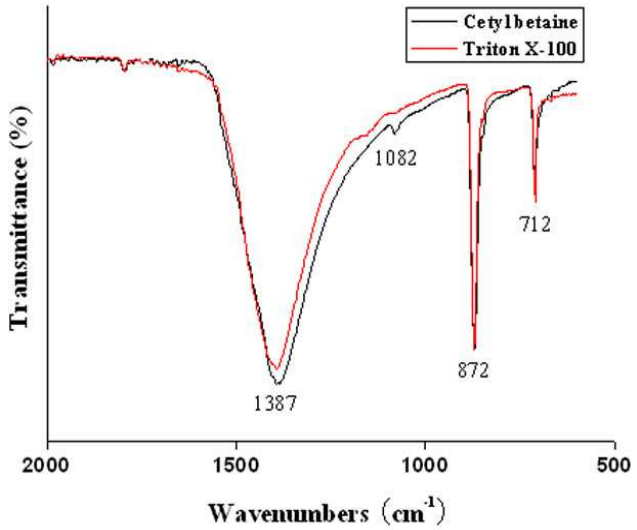

Figure 10. FTIR spectra of as-synthesized $CaCO_3$ fabricated on the cetyl betaine-assembled hydrophilic substrate (black line) and the Triton X-100-assembled hydrophilic substrate (red line) after 48h of mineralization.

What should also be mentioned is the *n*-hexane-aqueous interfaces we constructed. The amphipathic surfactants in the aqueous solution tend to aggregate at the interfaces to minimize the interfacial free energy. The concentration of the surfactants at the interfaces is higher than that of the bulk solution. Therefore, the surfactants micelles on the substrates will be kept intact when the surfactants micelles modified substrates were put at the interfaces. Besides, the use of the organic-inorganic interfaces is a way to mimic the bio systems because many organisms, including mollusks, echinoderms, calcisponges, corals, form their hierarchical mineral skeleton out of calcium carbonate minerals in the organic-inorganic interfaces. Also, the organic-inorganic interfaces have been proved to have outstanding advantages over the bulk aqueous solution in controlling the assembly of inorganic nanoparticles in the previous works.[43,44] Thus, this biomimetic approach will be promising in synthesizing other functional nanoparticles or nanodevices.

Conclusions

Combining the regulatory effect and the template role of surfactants, we use the surfactant micelles modified PET substrate to modulate the morphologies of $CaCO_3$ at the n-hexane-$Ca(OH)_2$ saturated solution interfaces. After 48h of crystallization, spherical and hexagonal $CaCO_3$ crystals with hierarchical structure were obtained separately by using different kinds of surfactants. During the crystal growth process, the assembled surfactant micelles not only contributed to stabilizing

the assembly of nanoparticles, but also exerted vigorous control over the morphology of the products. From the time dependent experiments, we suggest that $CaCO_3$ synthesis follows the nanoparticle-mediated self-organization processes. The organic-inorganic liquid interfaces brought about the controlled nucleation of calcite from ACC. The surfactant in solution induced the formation of $CaCO_3$ with well-defined orientation and morphology by specific adsorption. And the surfactant micelles on the substrate act as a template which allows further growth and decides the final hierarchical structure of the crystals. These findings will help for better understanding of the formation mechanism of the unique $CaCO_3$ morphologies. The biomimetic system will also contribute some valuable information to biomineralization researches.

Acknowledgment

This work is supported by the National Basic Research Program of China (973 Program) with No. 2011CB706900, the National Nature Science Foundation of China (nos. 50872149 and 50502003), the Scientific Research Foundation for Returned Scholars within the Ministry of Education of China, and the President Foundation of the Graduate University of the Chinese Academy of Sciences.

Notes and references

[a] *College of Materials Science and Opto-Electronic Technology, University of Chinese Academy of Sciences, Yuquan Road 19A, Beijing, 100049 China. Fax: 86 10 88256532; Tel: 86 10 88256532; E-mail: xiangjh@ucas.ac.cn*

[b] *College of Materials Science and Engineering, Taiyuan University of Technology, Taiyuan 030024, China. E-mail: liangxiaohong@tyut.edu.cn*

† Electronic Supplementary Information (ESI) available: The XRD pattern of blank PET substrate. The SEM image of crystals grown at the interface without surfactant in the inorganic phase for 48h. See DOI: 10.1039/b000000x/

‡ Footnotes should appear here. These might include comments relevant to but not central to the matter under discussion, limited experimental and spectral data, and crystallographic data.

1. R. A. Metzler, I. W. Kim, K. Delak, J. S. Evans, D. Zhou, E. Beniash, F. Wilt, M. Abrecht, J.-W. Chiou, J. Guo, S. N. Coppersmith and P. U. P. A. Gilbert, *Langmuir*, 2008, **24**, 2680-2687.
2. H. Colfen, *Nat Mater*, 2010, **9**, 960-961.
3. W. Dong, C. Tu, W. Tao, Y. Zhou, G. Tong, Y. Zheng, Y. Li and D. Yan, *Cryst. Growth Des.*, 2012, **12**, 4053-4059.
4. J. W. Nielsen, K. K. Sand, C. S. Pedersen, L. Z. Lakshtanov, J. R. Winther, M. Willemoës and S. L. S. Stipp, *Cryst. Growth Des.*, 2012, **12**, 4906-4910.
5. G. Begum and R. K. Rana, *Chem. Commun.*, 2012, **48**, 8216-8218.
6. Y. Fukui and K. Fujimoto, *J. Mater. Chem.*, 2012, **22**, 3493-3499.
7. J. Ihli, Y.-Y. Kim, E. H. Noel and F. C. Meldrum, *Adv. Funct. Mater.*, 2013, **23**, 1575-1585.
8. L. Liu, D. He, G.-S. Wang and S.-H. Yu, *Langmuir*, 2011, **27**, 7199-7206.
9. D. C. Bassett, B. Marelli, S. N. Nazhat and J. E. Barralet, *Adv. Funct. Mater.*, 2012, **22**, 3460-3469.
10. E. Asenath-Smith, H. Li, E. C. Keene, Z. W. Seh and L. A. Estroff, *Adv. Funct. Mater.*, 2012, **22**, 2891-2914.
11. H. Li and L. A. Estroff, *J. Am. Chem. Soc.*, 2007, **129**, 5480-5483.
12. J. Aizenberg, A. J. Black and G. M. Whitesides, *J. Am. Chem. Soc.*, 1999, **121**, 4500-4509.
13. B. Pokroy and J. Aizenberg, *Crystengcomm*, 2007, **9**, 1219-1225.
14. X. Liang, J. Xiang, F. Zhang, L. Xing, B. Song and S. Chen, *Langmuir*, 2009, **26**, 5882-5888.
15. A. S. Schenk, I. Zlotnikov, B. Pokroy, N. Gierlinger, A. Masic, P. Zaslansky, A. N. Fitch, O. Paris, T. H. Metzger, H. Cölfen, P. Fratzl and B. Aichmayer, *Adv. Funct. Mater.*, 2012, **22**, 4668-4676.
16. X. Wei, Y. Su, T. Wen, Z. Li, J. Yang and D. Wang, *Crystengcomm*, 2013, **15**, 3417-3422.
17. Z. Zhao, L. Zhang, H. Dai, Y. Du, X. Meng, R. Zhang, Y. Liu and J. Deng, *Microporous and Mesoporous Materials*, 2011, **138**, 191-199.
18. J. Aizenberg, N. Ilan, S. Weiner and L. Addadi, *Connect. Tissue Res.*, 1996, **35**, 17-23.
19. S. Elhadj, E. A. Salter, A. Wierzbicki, J. J. De Yoreo, N. Han and P. M. Dove, *Cryst. Growth Des.*, 2005, **6**, 197-201.
20. K. Naka, S.-C. Huang and Y. Chujo, *Langmuir*, 2006, **22**, 7760-7767.
21. Y. Liu, Y. Cui, H. Mao and R. Guo, *Cryst. Growth Des.*, 2012, **12**, 4720-4726.
22. Y.-Y. Kim, K. Ganesan, P. Yang, A. N. Kulak, S. Borukhin, S. Pechook, L. Ribeiro, R. Kröger, S. J. Eichhorn, S. P. Armes, B. Pokroy and F. C. Meldrum, *Nat Mater*, 2011, **10**, 890-896.
23. B. Xie, H. Shi, G. Liu, Y. Zhou, Y. Wang, Y. Zhao and D. Wang, *Chem. Mat.*, 2008, **20**, 3099-3104.
24. Y. Hou, M. Cao, M. Deng and Y. Wang, *Langmuir*, 2008, **24**, 10572-10574.
25. K. S. Varanasi and S. Garoff, *Langmuir*, 2005, **21**, 9932-9937.
26. H. Bock and K. E. Gubbins, *Phys. Rev. Lett.*, 2004, **92**, 135701.
27. R. Atkin and G. G. Warr, *J. Am. Chem. Soc.*, 2005, **127**, 11940-11941.
28. W. Mamdouh, H. Uji-i, J. S. Ladislaw, A. E. Dulcey, V. Percec, F. C. De Schryver and S. De Feyter, *J. Am. Chem. Soc.*, 2005, **128**, 317-325.
29. A. Guerrero-Martínez, J. Pérez-Juste, E. Carbó-Argibay, G. Tardajos and L. M. Liz-Marzán, *Angew. Chem.-Int. Edit.*, 2009, **48**, 9484-9488.
30. K. S. Choi, E. W. McFarland and G. D. Stucky, *Adv. Mater.*, 2003, **15**, 2018-2021.
31. K.-S. Choi, H. C. Lichtenegger, G. D. Stucky and E. W. McFarland, *J. Am. Chem. Soc.*, 2002, **124**, 12402-12403.
32. P. Zhu, M. Teranishi, J. Xiang, Y. Masuda, W.-S. Seo and K. Koumoto, *Thin Solid Films*, 2005, **473**, 351-356.
33. J. Xiang, P. Zhu, Y. Masuda and K. Koumoto, *Langmuir*, 2004, **20**, 3278-3283.
34. M.-H. Park, Y. Ofir, B. Samanta and V. M. Rotello, *Adv. Mater.*, 2009, **21**, 2323-2327.
35. S. Manne and H. E. Gaub, *Science*, 1995, **270**, 1480-1482.
36. Y. I. Rabinovich, S. Pandey, D. O. Shah and B. M. Moudgil, *Langmuir*, 2006, **22**, 6858-6862.
37. K. Shah, P. Chiu and S. B. Sinnott, *Journal of Colloid and Interface Science*, 2006, **296**, 342-349.
38. J. Ihli, A. N. Kulak and F. C. Meldrum, *Chem. Commun.*, 2013.
39. P. Bots, L. G. Benning, J.-D. Rodriguez-Blanco, T. Roncal-Herrero and S. Shaw, *Cryst. Growth Des.*, 2012, **12**, 3806-3814.
40. N. Gehrke, H. Cölfen, N. Pinna, M. Antonietti and N. Nassif, *Cryst. Growth Des.*, 2005, **5**, 1317-1319.
41. L. Addadi, S. Raz and S. Weiner, *Adv. Mater.*, 2003, **15**, 959-970.
42. A. Sarkar, K. Dutta and S. Mahapatra, *Cryst. Growth Des.*, 2012, **13**, 204-211.
43. Y. Lin, H. Skaff, T. Emrick, A. D. Dinsmore and T. P. Russell, *Science*, 2003, **299**, 226-229.
44. M. X. Luo, Y. M. Song, and L. L. Dai, *J. Chem. Phys.*, 2009,**131**, 194703.